Suppression of MicroRNA-9 by Mutant EGFR Signaling Upregulates FOXP1 to Enhance Glioblastoma Tumorigenicity

German G. Gomez[1], Stefano Volinia[2], Carlo M. Croce[2], Ciro Zanca[1], Ming Li[3], Ryan Emnett[4], David H. Gutmann[4], Cameron W. Brennan[5], Frank B. Furnari[1], and Webster K. Cavenee[1]

Abstract

The EGF receptor (EGFR) is amplified and mutated in glioblastoma, in which its common mutation (ΔEGFR, also called EGFRvIII) has a variety of activities that promote growth and inhibit death, thereby conferring a strong tumor-enhancing effect. This range of activities suggested to us that ΔEGFR might exert its influence through pleiotropic effectors, and we hypothesized that microRNAs might serve such a function. Here, we report that ΔEGFR specifically suppresses one such microRNA, namely miR-9, through the Ras/PI3K/AKT axis that it is known to activate. Correspondingly, expression of miR-9 antagonizes the tumor growth advantage conferred by ΔEGFR. Silencing of FOXP1, a miR-9 target, inhibits ΔEGFR-dependent tumor growth and, conversely, de-repression of FOXP1, as a consequence of miR-9 inhibition, increases tumorigenicity. FOXP1 was sufficient to increase tumor growth in the absence of oncogenic ΔEGFR signaling. The significance of these findings is underscored by our finding that high FOXP1 expression predicts poor survival in a cohort of 131 patients with glioblastoma. Collectively, these data suggest a novel regulatory mechanism by which ΔEGFR suppression of miR-9 upregulates FOXP1 to increase tumorigenicity. *Cancer Res; 74(5); 1429–39. ©2014 AACR.*

Introduction

Glioblastomas infiltrate normal brain parenchyma, display a high degree of cellular and genetic intratumoral heterogeneity, and exhibit limited responses to conventional therapies (1). Molecular analyses have shown that 40% to 50% of primary glioblastomas have EGFR amplification, overexpression, and/or mutations (2). The most common EGFR mutant, ΔEGFR (also known as EGFRvIII and de2-7), is generated from an in-frame 801-bp deletion of exons 2–7 (3), and is constitutively active and present in a high proportion of glioblastomas with EGFR amplification (2). ΔEGFR confers a variety of biologic effects upon its expression, including resistance to radiation (4) and chemotherapeutic agents (5), promotion of tumor cell motility and invasion (6), enhancement of tumorigenicity *in vivo* (7), maintenance of glioblastoma growth (8), and heterogeneity (9). Collectively, this broad spectrum of biologic activities provides a compelling rationale for the molecular targeting of EGFR in glioblastoma.

MicroRNAs (miRNA) are a group of non–protein-encoding RNAs of 19–25 nt in length that block translation or facilitate mRNA degradation upon binding to complementary sequences in the 3′ UTR of their target mRNAs (10). miRNA biogenesis is initiated upon the processing of primary transcripts by Drosha/DGCR8 complexes to yield 60–110 nt long hairpins containing precursor miRNAs (11). After export of the pre-miRNAs to the cytoplasm by exportin-5 (12), mature miRNAs are excised from the pre-miRNAs by the RNase III enzyme, Dicer (13), and loaded into the RNA-induced silencing complex (RISC; ref. 14). Within the RISC, mature miRNAs are guided to their appropriate target mRNAs to prevent translation. miRNAs are highly conserved among distant species and are involved in many biologic processes, including cancer initiation, maintenance, and progression (15).

Dysregulation of miRNA expression in cancers occurs through multiple mechanisms such as genomic alterations (15), miRNA gene methylation (15), aberrant transcription (16), and defective miRNA processing (15). Highlighting the importance of miRNAs in regulating the pathogenic effects of growth factor receptor signaling in glioblastoma, miRNAs targeting oncogenic receptors such as EGFR, PDGFR, and c-MET inhibit the invasion, proliferation, tumorigenicity, and gliomagenesis induced by these receptors (17–19). Providing an example of a miRNA-dependent feedback mechanism in controlling growth factor receptor signaling, platelet-derived growth factor (PDGF)-induced suppression of EGFR activation requires miR-146b activity (20).

In this report, we sought to determine whether miRNAs act as downstream effector molecules that regulate the oncogenic

Authors' Affiliations: [1]Ludwig Institute for Cancer Research, University of California San Diego, La Jolla, California; [2]Department of Molecular Virology, Immunology and Medical Genetics, Comprehensive Cancer Center, The Ohio State University, Columbus, Ohio; [3]Department of Human and Molecular Genetics, Virginia Commonwealth University School of Medicine, Richmond, Virginia; [4]Department of Neurology, Washington University School of Medicine, St. Louis, Missouri; and [5]Department of Neurosurgery, Memorial Sloan-Kettering Cancer Center, New York, New York

Note: Supplementary data for this article are available at Cancer Research Online (http://cancerres.aacrjournals.org/).

Corresponding Author: Frank B. Furnari, Ludwig Institute for Cancer Research, University of California at San Diego, 9500 Gilman Dr, CMM-East Room 3055, La Jolla, CA 92093-0660. Phone: 858-534-7819; Fax: 858-534-7750; E-mail: ffurnari@ucsd.edu

doi: 10.1158/0008-5472.CAN-13-2117

effects exerted by aberrant EGFR signaling in glioblastoma. Collectively, our data suggest that the suppression of miR-9 by the ΔEGFR/Ras/PI3K/AKT axis provides a tumor growth advantage to ΔEGFR-driven tumors through the upregulation of the transcription factor, FOXP1. Silencing of FOXP1 inhibited the growth of ΔEGFR-driven tumors. Upregulation of FOXP1, as a consequence of inhibiting miR-9 activity, increased the tumorigenicity of glioblastoma cells, suggesting that miR-9 is a tumor suppressor, whereas FOXP1 likely functions as an oncogenic factor in glioblastoma. Finally, high FOXP1 expression was significantly associated with poor survival in patients with glioblastoma, further supporting the hypothesis that FOXP1 is an oncogenic driver downstream of EGFR signaling.

Materials and Methods

Cell culture

U87 and U373 parental glioma cells and those expressing wild-type EGFR (WT EGFR), ΔEGFR and dead kinase ΔEGFR (DK), and the U87Δ DY mutants were cultured as described (7, 21). LN229, U178, U251, and mouse *Ink4a/Arf*$^{-/-}$/*Pten*$^{-/-}$ astrocytes were maintained in Dulbecco's Modified Eagle Medium (DMEM) containing 10% FBS (22). Mouse *Ink4a/Arf*$^{-/-}$/*Pten*$^{-/-}$ astrocytes expressing ΔEGFR were maintained in DMEM supplemented with 1 μg/mL puromycin (22). Primary murine astrocyte cultures were established from the brainstems of postnatal day 1–2 mouse *Nf1*$^{flox/flox}$ pups, as described previously (23). WT and *Nf1*-deficient (*Nf1*$^{-/-}$) cultures were generated following infection with Adenovirus type 5 containing β-galactosidase (Ad5-LacZ) or Cre recombinase (Ad5-Cre; University of Iowa Gene Transfer Vector Core, Iowa City, IA), respectively.

miRNA microarray hybridization, quantification, and analysis

Glioma cells were starved 48 hours before total RNA extraction using TRIzol (Life Technologies). RNA labeling and hybridization to miRNA microarray chips was performed as described (24). In brief, 5 μg of total RNA from each sample was reverse transcribed using biotin end-labeled random-octamer oligonucleotide primers. Hybridization of biotin-labeled cDNA was performed on the new Ohio State University custom miRNA microarray chip (OSU_CCC version 3.0), which contains approximately 1,100 miRNA probes, including 326 human and 249 mouse miRNA genes, spotted in duplicates. The hybridized chips were washed and processed to detect biotin-containing transcripts by streptavidin-Alexa647 conjugate and scanned on an Axon 4000B microarray scanner (Axon Instruments). Hybridization signals were quantified using the GenePix 6.0 software (Axon Instruments). Average values of replicate spots of each miRNA were background subtracted, quantile normalized, and subjected to further analysis (GEO accession: GSE53504).

Northern blotting

Total RNA (10–20 μg) was diluted with 2× RNA sample loading buffer (95% formamide, 18 mmol/L EDTA, 0.25% SDS, 0.25% xylene cyanol, and 0.25% bromophenol blue), denatured at 95°C for 5 minutes, and separated on 15% polyacrylamide gels containing 8 mol/L urea. The RNA was transferred to positively charged nylon membranes (GE Healthcare Bio-Sciences Corp) in 0.5× TBE using the Trans-Blot SD semi-dry electrophoretic transfer cell (Bio-Rad) and crosslinked to blots by UV irradiation (Stratagene). Blots were prehybridized for 1 hour in ULTRAhyb-Oligo buffer (Life Technologies) at 30°C. DNA probes were ^{32}P-labeled using the StarFire MiRNA Detection Kit (Integrated DNA Technologies), diluted into 10 mL ULTRA-hyb oligo buffer and hybridized to the membranes overnight at 30°C. Blots were washed twice for 30 minutes with 50 mL of 2× SSC containing 0.5% SDS at 30°C and exposed to phosphor imaging screens (Bio-Rad). The miRNA and reference small RNA signals were obtained with the Personal Molecular Imager (Bio-Rad) and quantified with Quantity One Software (Bio-Rad). Blots were stripped in boiling 0.1% SDS for 15 minutes and allowed to cool to room temperature before reprobing. Probe sequences were, miR-9: 5′-TCA TAC AGC TAG ATA ACC AAA GA-3′, miR-9*: 5′-ACT TTC GGT TAT CTA GCT TTA T-3′, U44: 5′-CAT TTG CTA TCA TCA TCC AGG-3′, and snoRNA 202: 5′-CTT TCA TCA AGT CAG TAC AGC-3′.

Quantitative real-time PCR

cDNA was synthesized from 1 μg of DNase I–treated RNA using the SuperScript III First-Strand Synthesis SuperMix for qPCR Kit (Life Technologies). Triplicate quantitative real-time PCR (qRT-PCR) reactions were run for each sample using iQ SYBR Green Supermix and the iQ5 cycler (Bio-Rad). The following reaction conditions were used: 95°C for 5 minutes, 40 cycles of 95°C for 15 seconds, and 58°C for 60 seconds. Data were normalized to the reference gene, GAPDH, and relative expression determined using the $2^{-\Delta\Delta Ct}$ formula. The primer sequences used to amplify hsa-pri-miR-9-1, hsa-pri-miR-9-2, and hsa-pri-miR-9-3 were as described previously (25). Mature miRNA expression was determined using small RNA TaqMan assays according to manufacturer's instructions (Life Technologies).

Growth factor stimulations and inhibitor studies

Recombinant EGF (50 ng/mL, R&D Systems) was added to U87WT and U87Δ EGFR cells for the different lengths of time 48 hours after serum starvation. HGF (20 ng/mL, PeproTech), PDGF-BB (50 ng/mL, PeproTech), and bFGF (20 ng/mL, PeproTech) and heparin (5 μg/mL, STEMCELL Technologies) were added to serum-starved U87 cells for 24 hours. Following 24-hour serum starvation, U87ΔEGFR were incubated with 5 μmol/L of a Raf kinase inhibitor (EMD Millipore) for 24 hours. ΔEGFR kinase activity was inhibited by treating serum-starved cells with 0.5 to 1 μmol/L gefitinib (LC Laboratories) for 24 to 48 hours.

Western blotting

Western blotting was performed as described previously (26). Antibodies used in this study were as follows: anti-phosphotyrosine clone 4G10 antibody was obtained from EMD Millipore; anti-FOXP4 was from Bethyl Labs, anti–phospho-Akt, total Akt, phospho-ERK, total ERK, SOS1, phospho-S6 ribosomal protein, S6 ribosomal protein, and FOXP1 were

obtained from Cell Signaling Technology; and PTEN and β-actin were from Santa Cruz Biotechnology.

RNAi studies

SOS1 siRNAs and control siRNAs were obtained from Sigma-Aldrich and Santa Cruz Biotechnology. Cells were reverse transfected with 20 nmol/L of siRNA duplexes using Lipofectamine RNAiMAX (Invitrogen) according to the manufacturer's instructions. RNA and protein lysates were collected 48 hours after transfection.

RNA ligase-mediated rapid amplification of cDNA ends

To map the 5′ end of the host gene of pri-miR-9-2, RLM-RACE was accomplished using the GeneRacer Kit (Life Technologies). In brief, 5 μg of total RNA extracted from U87 cells was reverse transcribed using the SuperScript III RT enzyme reagents (Life Technologies). cDNA was amplified with the Expand Long Template PCR System (Roche Applied Science), GeneRacer 5′ primer, the miR-9-2 gene-specific reverse primer, 5′- CAT TCT CAC ACG CTC CCC GGC GAT CT -3′, and the nested reverse miR-9-2 primer, 5′-CAT TCT CAC ACG CTC CCC GGC GA -3′. PCR products were cloned using the TOPO TA Cloning Kit (Life Technologies), sequenced, and aligned with Ref Seq RNAs (Feb 2009 GRCh37/hg19 assembly) using the UCSC Genome Browser to LINC00461 variant 1 (chr5: 87,960,263- 87,969,146).

Retroviral transductions

To produce retrovirus, 293T cells were transfected with pSuper-puro, pSuper-puro miR-9-1, pBABE-puro, pBABE-puro G129R PTEN, pBABE-puro PTEN, pBABE-puro kinase-dead Akt, MDH1-PGK-GFP-MIR-9 (Addgene, plasmid #25036), MDH1-PGK-GFP-2.0 (Addgene, plasmid #11375), pwzl-hygro (Addgene, plasmid #18750), and pwzl-HRas G12V (Addgene, plasmid #18749) together with pCL10A1 using Lipofectamine 2000 (Invitrogen). To produce lentiviruses, 293FT cells were cotransfected with pLKO.1-puro, pLKO.1-puro shFOXP1 (Sigma-Aldrich), miRZip control and miRZip-miR-9 (System Biosciences) together with pCMVDR8.91 and pMD.G-VSV-G using Lipofectamine 2000. Viral supernatants were filtered at 48 and 72 hours after transfection. For knockdown of the LINC00461 variant 1, the following oligonucleotides were synthesized and cloned into pLKO.1-puro: forward oligo-5′ CCGG TCTCAGC-TAGATGGGTCTAAACTCGAGTTTAGACCCATCTAGCTGAG-ATTTTTG-3′; reverse oligo-5′ AATTCAAAAATCTCAGCTAG-ATGGGTCTAAACTCGAGTTTAGACCCATCTAGCTGAGA-3′. Glioma cells were infected overnight in the presence of 8 μg/mL polybrene and then selected for 3 days in DMEM containing 2 μg/mL puromycin. The stable clones were verified by Western blot analysis and qRT-PCR.

Luciferase reporter assays

The FOXP1 3′ UTR, a miR-9 full-length binding site (23 nt) and a mutant miR-9 binding site with 4 mismatched nucleotides were cloned between the *Xho*1 and *Not*1 restrictions sites of the psiCHECK-2 reporter plasmid (Promega). Between 5×10^4 and 1×10^5 cells were plated into 24-well plates. Cells were cotransfected with 100 ng reporter plasmid and 100 nmol/L microRNA mimics (Sigma-Aldrich) or 100 nmol/L miR-9 Locked Nucleic Acids (Exiqon Inc.). Relative luciferase activity was determined 30 hours after transfection.

In vivo tumorigenicity assays

Athymic nude mice 4 to 5 weeks of age were injected with 2.5×10^5 U87ΔEGFR cells suspended in 0.1 mL of PBS on each flank (5×10^5 total cells per mouse). Tumor width (a) and length (b) were obtained using calipers and tumor volumes determined using the formula $V = {}^1/_2 \times a \times b^2$, where $b \leq a$. Mice were euthanized when tumor volumes exceeded 1,500 mm^3 or tumors became ulcerated, as directed by our institutional guidelines for animal welfare and experimental conduct. For tumorigenicity assays examining tumor growth kinetics upon inhibition of miR-9 activity or overexpression of FOXP1, mice were injected with 1×10^6 to 5×10^6 cells on each flank and tumor volumes determined as described above.

Statistical analysis

All data were analyzed for significance using KaleidaGraph software, where $P \leq 0.05$ was considered statistically significant. One-way ANOVA, the Kruskal–Wallis test, the Mann–Whitney test, and two-tailed t tests were used to compare groups. False discovery rate (FDR) was used to control for multiple testings. A Kaplan–Meier curve for a cohort of 131 patients with glioblastoma was generated using Probe Set Analyzer (http://probesetanalyzer.com). The patient cohort is composed of 67 newly diagnosed cases of glioblastoma and 64 cases of recurrent glioblastoma with 80 patients being $\geq$50 years and 51 patients $\leq$50 years of age. The probe set for FOXP1 was retrieved and normalized expression levels adjusted to group patients into low (normalized expression intensity range 46–102) and high (normalized expression intensity range 173-528) FOXP1 expression categories.

Results

ΔEGFR suppresses miR-9

To identify miRNAs regulated by EGFR, RNA from 2 different glioma cell lines (U87 and U373) were hybridized to miRNA expression arrays and analyzed. Each cell type was engineered to express wild-type EGFR (WTEGFR), dead kinase ΔEGFR (DK), or ΔEGFR at elevated levels, similar to those observed in primary glioblastomas displaying EGFR overexpression (7). Parental cells expressing endogenous EGFR and WTEGFR cells stimulated with EGF for 1 hour were also included in the analyses. We reasoned that 1 hour of EGF stimulation was appropriate given that 20 minutes of EGF stimulation is sufficient to induce or suppress miRNA expression in breast and brain tumor cells (27).

In agreement with prior studies, four different glioma cell types analyzed showed high expression of miR-21, miR-221, and miR-26a as well as low miR-124, miR-137, miR-219-5p, miR-34a, and miR-7 expression (Supplementary Table S1; ref. 28). Our data revealed that the different cell lines displayed dramatically distinct miRNA profiles (Supplementary Table S1). Likely, as a result of the distinct miRNA profiles displayed by the cell lines, we did not identify a common miRNA, or group of miRNAs, regulated by EGF in U87 an U373 cells. We also did

Table 1. List of microRNAs putatively regulated by ΔEGFR

P[a]	ΔEGFR[b]	Others[b]	Fold change[c]	microRNA[d]
0.00005	1,773	1,421	1.3	hsa-miR-320
0.00010	1,868	1,471	1.3	hsa-miR-373*
0.00015	2,139	1,660	1.3	hsa-miR-24
0.00005	430	739	−1.7	hsa-miR-181c
0.00016	933	1,273	−1.4	hsa-miR-181a
0.00091	103	405	−3.9	hsa-miR-9
0.00110	17	49	−2.9	hsa-miR-32
0.00396	2,728	3,449	−1.3	hsa-miR-181b
0.00538	566	763	−1.3	hsa-miR-10b
0.00642	15	25	−1.7	hsa-miR-424*

[a]*P* values of microRNAs demonstrating significant differences in expression at the nominal 0.01 level of the univariate test. FDR threshold was ≤ 0.05.

[b]Geometric mean intensity values obtained from microRNA arrays are given for each group. Mean intensity of others group represents parental cells, cells expressing WT and DK EGFR, and WT cells stimulated with EGF for 1 hour.

[c]Fold change in microRNA expression in ΔEGFR cells relative to other cell types.

[d]The symbol "*" denotes those mature miRNAs showing reduced expression relative to miRNAs generated from opposite stands of the same pre-miRNA hairpin. miRNAs with almost identical sequences are annotated with a lowercase letter. For example, hsa-miR-181a, hsa-miR-181b, and hsa-miR-181c are highly similar in sequence.

not find a miRNA regulated in a similar manner by activated WTEGFR and ΔEGFR. Given that ΔEGFR signaling is distinct from WTEGFR signaling (29), we analyzed the data to identify miRNAs whose levels were changed in cells expressing ΔEGFR as compared with those expressing the other receptor types. We identified 10 miRNAs that were differentially expressed in ΔEGFR cells relative to parental, DK, WTEGFR, and WTEGFR cells stimulated with EGF (Table 1). Most of these miRNAs showed small expression changes and we focused on miR-9 because it displayed a 3.9-fold downregulation in ΔEGFR cells (Table 1). We then validated the downregulation of miR-9 in U87 and U373 ΔEGFR cells (Fig. 1A and B) by direct Northern blotting. Interestingly, mouse *Ink4a/Arf*$^{-/-}$*/Pten*$^{-/-}$ astrocytes engineered with ΔEGFR (astrocytes Δ) showed decreased miR-9 expression relative to the control astrocytes, suggesting a conserved cross-species mechanism of miR-9 regulation (Fig. 1c). In addition, inhibition of ΔEGFR signaling with gefitinib, an EGFR tyrosine kinase inhibitor, upregulated miR-9 expression, validating that miR-9 is regulated by ΔEGFR kinase activity (Fig. 1D).

Because it was plausible for sustained signaling through WTEGFR to inhibit miR-9 expression, we determined miR-9 expression after treating U87WTEGFR cells with EGF for different lengths of time. While ΔEGFR suppressed miR-9, prolonged activation of WTEGFR did not show a similar modulation of miR-9 expression (Fig. 1e). We also observed that treatment of U87 cells with EGF, PGDF-β, bFGF, and HGF for 24 hours did not significantly affect miR-9 expression (Supplementary Fig. S1A). Moreover, treatment of U87ΔEGFR cells with EGF did not affect miR-9 expression (Supplementary Fig. S1B), suggesting that the downstream signaling components utilized by ΔEGFR to suppress miR-9 are not likely utilized to the same degree nor in the same manner by activated WTEGFR. Collectively, these data show that ΔEGFR signaling negatively regulates miR-9 expression.

ΔEGFR negatively regulates pri-miR-9-2

We next sought to clarify the step at which ΔEGFR disrupts miR-9 biogenesis. In cancer cells, alterations of miRNA biogenesis have been shown to occur through transcriptional dysregulation of miRNA host genes, changes in the rates of processing precursor miRNAs to mature miRNAs, and degradation of pre-miRNAs (15). In humans and mice, three primary transcripts (pri-miR-9-1, pri-miR-9-2, and pri-miR-9-3; ref. 25) are processed to give rise to mature miR-9. We first examined the relative expression levels of the miR-9 encoding primary transcripts in human normal brain tissue and U373 and U87 cells. Normal human brain expression of all three transcripts was detected at relatively low cycle threshold values by qRT-PCR (Supplementary Table S2). In contrast, only pri-miR-9-2 was expressed at high levels and reliably detected in U87 and U373 cells. Examination of human and mouse pri-miR-9-2 expression revealed that ΔEGFR downregulates pri-miR-9-2 (Fig. 2A). These data indicated that the downregulation of miR-9 was due to negative transcriptional regulation of pri-miR-9-2 by ΔEGFR, rather than alterations in miR-9 processing (30). To rule out pri-miR-9-2 degradation as the mechanism for miR-9 suppression by ΔEGFR, pri-miR-9-2 expression was determined after 6-hour treatment of U373 and mouse astrocyte parental and ΔEGFR cells with the transcriptional inhibitor, actinomycin D, which illustrated that ΔEGFR did not increase the rate of pri-miR-9-2 degradation (Fig. 2B). As the processing of pri-miR-9-2 gives rise to two mature miRNAs, miR-9 and miR-9*, we reasoned that miR-9* should also be downregulated by ΔEGFR. Indeed, miR-9* downregulation was displayed by ΔEGFR human glioblastoma cells and mouse astrocytes (Fig. 2C).

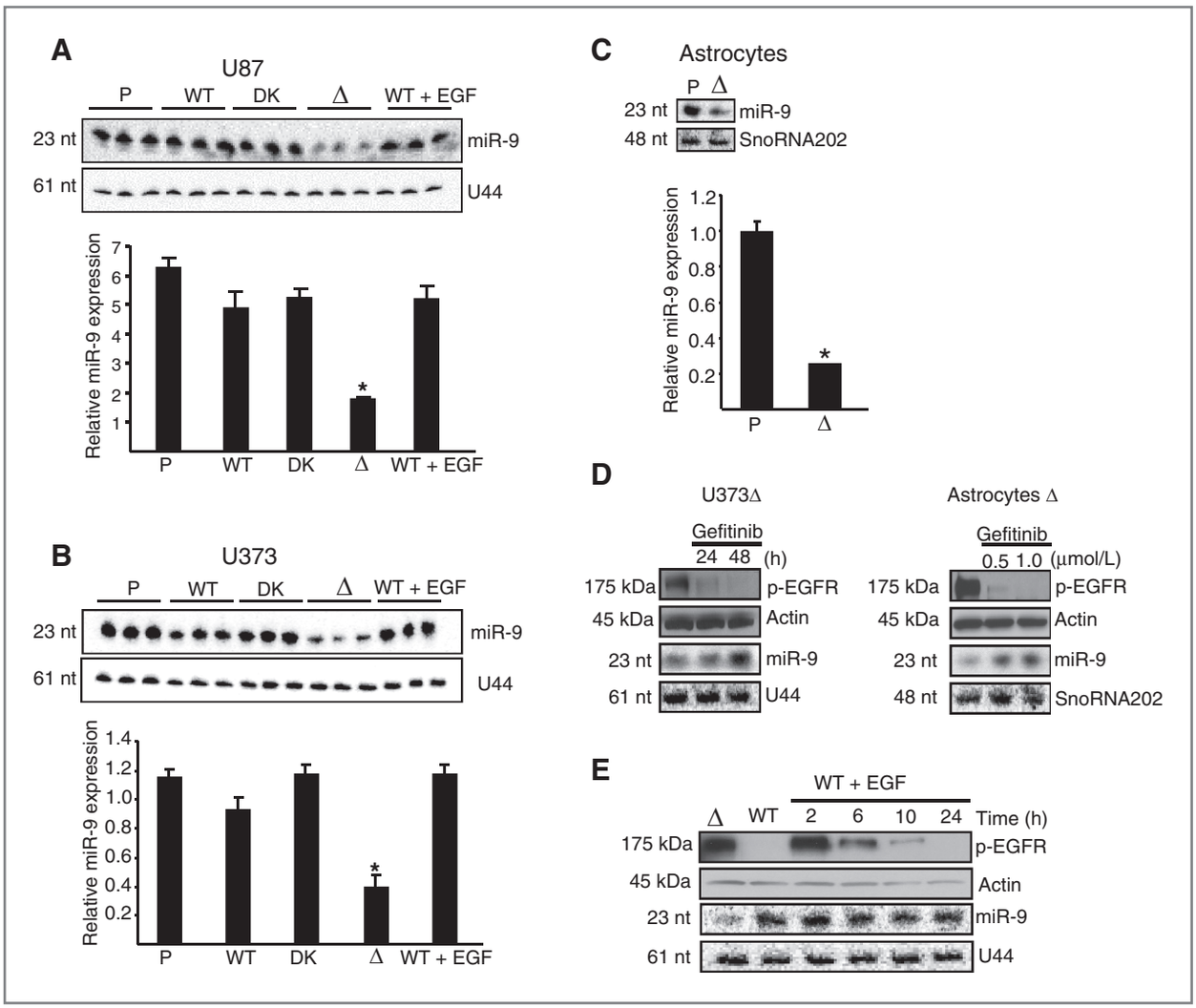

Figure 1. Validation of miR-9 repression by ΔEGFR. A and B, Northern blotting for miR-9 in triplicate glioma cell extracts validates the downregulation of miR-9 in U87 and U373 ΔEGFR cells (*, $P \leq 0.001$). C, Northern blotting and qRT-PCR show miR-9 downregulation in mouse ΔEGFR expressing astrocytes (*, $P \leq 0.002$). D, inhibition of ΔEGFR kinase activity in U373Δ cells (left, 1 μmol/L gefitinib) and astrocytes Δ (right, 0.5 and 1 μmol/L treated) induces miR-9 expression. E, prolonged stimulation of U87WTEGFR cells with EGF does not suppress miR-9 expression.

The Ras/PI3K/AKT axis suppresses miR-9

To further determine the signaling pathway components involved in regulating miR-9 downstream of ΔEGFR, we analyzed the levels of miR-9 in U87 cells expressing ΔEGFR mutants bearing tyrosine to phenylalanine (Y→F) substitutions that disrupt the binding of adaptor proteins to ΔEGFR (21). The U87DY1 (Y1173F) and U87DY2 (Y1068/1173F) mutants showed no change in miR-9 expression relative to control U87ΔEGFR cells (Fig. 3A). However, miR-9 was upregulated in the U87DY5 (Y992/1068/1086/1148/1173F) mutant (Fig. 3a). We have previously shown that Ras activity is elevated in U87ΔEGFR cells (21). Given that the U87DY5 and U87dead kinase ΔEGFR (DK) mutants are defective in binding to Grb2 and Shc and thus impaired in their ability to interact with Ras (21), relative to U87DY1, U87DY2, and control U87ΔEGFR cells, we hypothesized that Ras activity is required to suppress miR-9. To test this hypothesis, we first silenced the SOS1-positive regulator of Ras activity, in U87ΔEGFR cells and, as would be predicted, SOS1 silencing induced miR-9 expression (Fig. 3b). Introduction of an active mutant H-Ras allele, G12V, into parental U87 and U373 cells also increased Ras expression and activity, as indicated by the increased activation of AKT and ERK relative to control cells (Fig. 3c) and Ras activity was sufficient to suppress miR-9 expression (Fig. 3c). Repression of miR-9 was not observed in *Nf1*-null murine astrocytes relative to normal astrocytes, suggesting that activation of Ras, as a consequence of *Nf1* gene inactivation (31), is not sufficient to suppress miR-9 in untransformed astrocytes (Supplementary Fig. S2A). Supporting Ras involvement in repressing miR-9 in transformed astrocytes is information derived from analysis of The Cancer Genome Atlas (TCGA) glioblastoma dataset that showed that miR-9 expression is lower in the mesenchymal

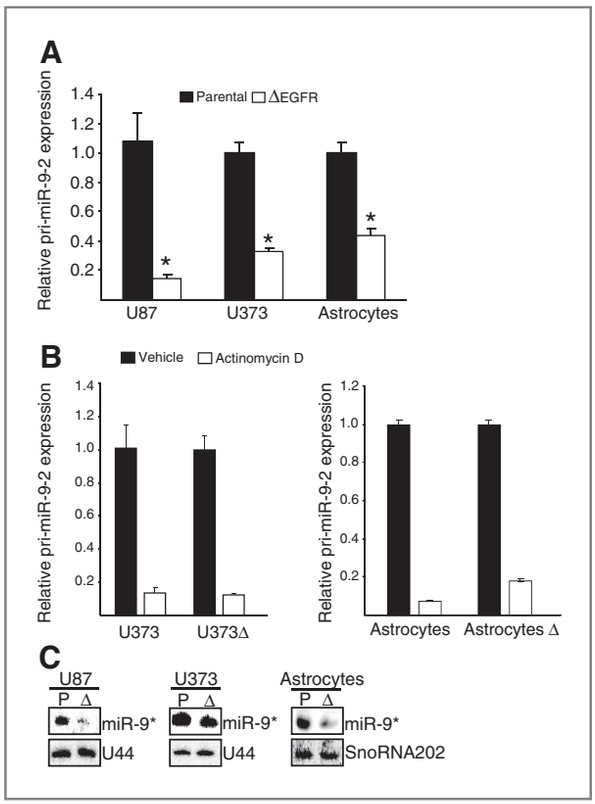

Figure 2. ΔEGFR downregulates pri-miR-9-2. A, ΔEGFR negatively regulates expression of the mouse and human primary transcript, pri-miR-9-2, encoding for miR-9 (*, $P \leq 0.001$). B, the rate of pri-miR-9-2 degradation is not accelerated by ΔEGFR. miR-9 expression was analyzed in U373 cells and mouse astrocytes treated for 6 hours with actinomycin C to block transcription. C, ΔEGFR downregulates miR-9* expression. Northern blotting revealed the suppression of miR-9*, generated from pri-miR-9-2, in ΔEGFR cells.

glioblastoma subtype known to show loss, mutation and/or decreased expression of the *Nf1* tumor suppressor gene (Supplemental Fig. S2B).

To determine the pathway downstream of Ras required for suppressing miR-9, we inhibited either the Ras/Raf/MEK/ERK or the Ras/PI3K/AKT axis. Inhibitor-mediated blockade of Raf1 in U87ΔEGFR cells had no effect on miR-9 levels (Fig. 3D), whereas disruption of PI3K activity by exogenous expression of PTEN in U87ΔEGFR cells caused upregulated miR-9 expression relative to cells infected with catalytically inactive PTEN (Fig. 3D). Finally, infection of U87ΔEGFR cells with dead kinase AKT also upregulated miR-9 (Fig. 3D). Overall, these data show that the Ras/PI3K/AKT axis suppresses miR-9.

miR-9 targets FOXP1

A limited number of miR-9 targets have been identified in glioblastoma cells to date (32, 33). Western blotting of some of the validated glioma-associated miR-9 targets revealed no correlation between target expression levels and miR-9 levels in ΔEGFR cells relative to parental cells (data not shown). Consequently, we used starBase (34) to identify novel miR-9 targets in glioblastoma, reasoning that starBase would significantly reduce the rate of false positive predictions because it integrates data from 21 high-throughput CLIP-Seq experiments with miRNA target sites predicted from 6 target prediction programs (34). The intersection of CLIP-seq data with target sites predicted by TargetScan and PicTar yielded a list of 30 putative miR-9 targets (Supplementary Table S3). Because miRNAs often induce target mRNA degradation, the mean signal obtained from probes on Affymetrix GeneChip Genome U133A arrays (6) for each putative target from U87ΔEGFR cells was divided by the mean signal from U87DK cells. Four putative targets showing a Δ/DK ratio $\geq$1.5 were selected for validation by qPCR, as well as seven putative targets not represented on the Affymetrix arrays (Supplementary Table S3). As none of the screened targets were significantly altered at the mRNA level, we reasoned that miR-9 likely blocks translation of its targets as previously reported (35). We deemed FOXP family members to be prime candidates as the FOXP1 and FOXP4 3′UTRs contain two predicted miR-9–binding sites. As Western blotting did not reveal an inverse correlation of miR-9 and FOXP4 expression levels (Supplementary Fig. S3) in U87 and U373DK cells relative to U87 and U373 ΔEGFR cells, we focused on FOXP1 given that miR-9 regulates FOXP1 in neurons (35). Western blotting revealed that FOXP1 expression was higher in human and mouse (U87, U373, and mouse astrocytes) ΔEGFR cells displaying low miR-9 expression relative to parental U373 cells and mouse astrocytes or U87DK cells with high miR-9 expression (Fig. 4A). Overexpression of miR-9 in U87ΔEGFR cells and astrocytes Δ caused downregulation of FOXP1 (Fig. 4B). Conversely, transduction of U87 cells with a miRZip miR-9 vector, designed to produce antisense RNA to inactivate miR-9, induced FOXP1 expression (Fig. 4C). To show a direct interaction between miR-9 and FOXP1, the 3′UTR of FOXP1 was cloned into a luciferase reporter vector and cells were cotransfected with the FOXP1 reporter vector and a non-specific miRNA mimic or a miR-9 mimic. Transfection of U87Δ cells with the miR-9 mimic significantly repressed FOXP1 reporter activity relative to cells transfected with the control miRNA mimic (Fig. 4D). Inhibition of miR-9 activity in U373 cells using anti–miR-9 locked nucleic acids induced a derepression of the luciferase activity of the FOXP1 reporter (Fig. 4E). Collectively, these data indicate that FOXP1 is a miR-9 target in glioblastoma cells.

miR-9 and FOXP1 regulate tumorigenicity

ΔEGFR confers an increased *in vivo* tumorigenic capacity to glioblastoma cells (7, 8). The suppression of miR-9 by ΔEGFR suggested the possibility that miR-9 might antagonize the tumor growth advantage conferred by ΔEGFR signaling. To test this, U87ΔEGFR cells stably overexpressing miR-9 were subcutaneously implanted into nude mice (Fig. 5A). Vector control U87ΔEGFR tumors were significantly larger than tumors formed by U87DK (Fig. 5A). U87ΔEGFR tumors overexpressing miR-9 were similar in size to U87DK tumors (Fig. 5A) and significantly smaller than U87 ΔEGFR tumors, indicating that miR-9 antagonizes the increased tumorigenicity conferred to glioblastoma cells by ΔEGFR.

The data also suggested that miR-9 might negatively regulate the tumorigenic capacity of glioblastoma cells lacking

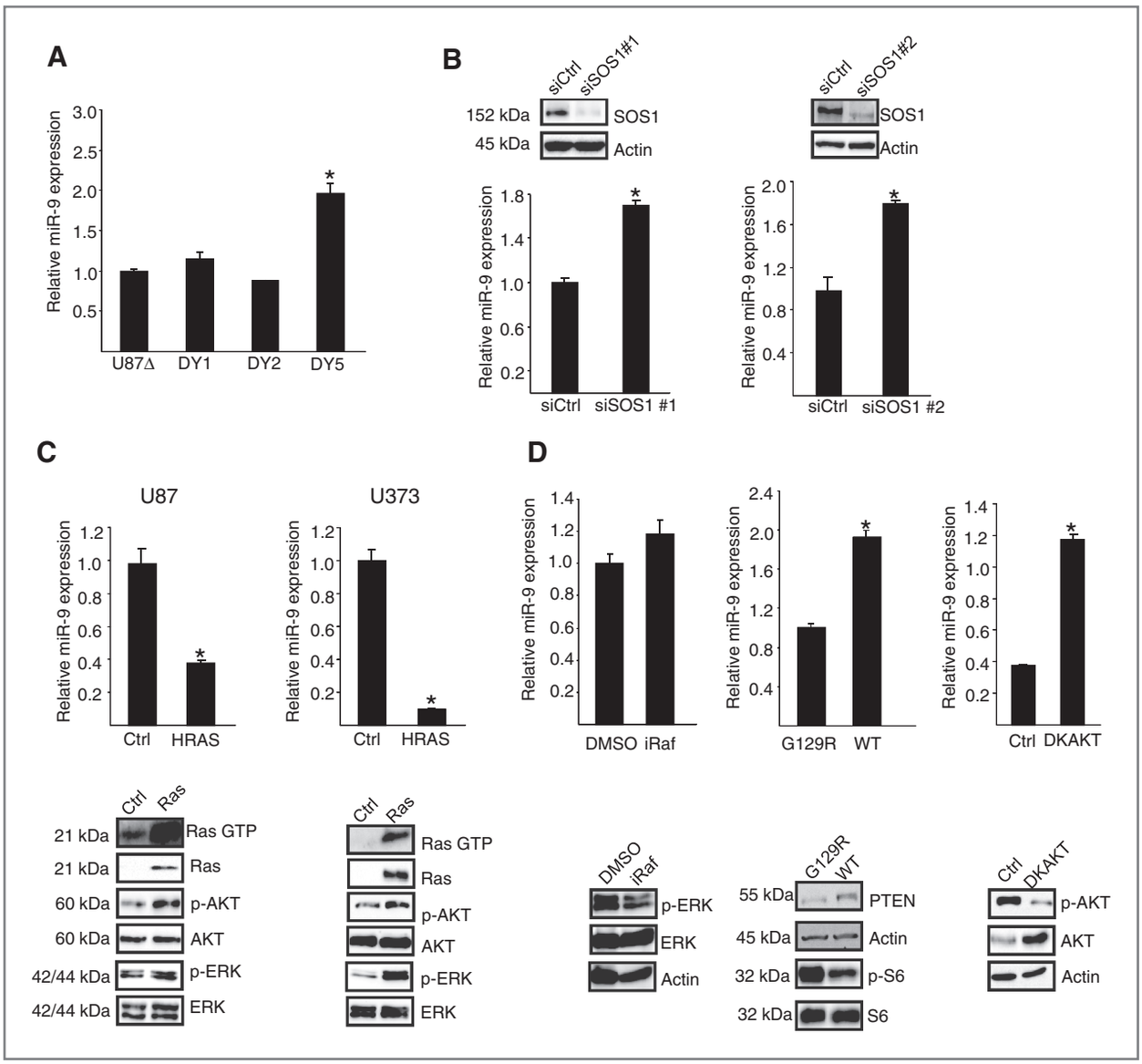

Figure 3. The Ras/PI3K/AKT axis is required for miR-9 repression. A, miR-9 expression was determined in cells with mutant ΔEGFR alleles bearing tyrosine to phenylalanine substitutions. The U87DY5 mutant with impaired binding to Ras shows upregulation of miR-9 (*, $P \leq 0.005$). B, SOS1 silencing upregulates miR-9 in U87ΔEGFR cells (*, $P \leq 0.004$). C, H-Ras G12V suppresses miR-9 (*, $P \leq 0.006$). D, treatment of U87ΔEGFR cells with a Raf inhibitor does not modulate miR-9 (left). D, introduction of wild-type PTEN (*, $P \leq 0.004$) or dead kinase AKT (DKAKT; *, $P \leq 0.04$) relieved the suppression of miR-9 in U87ΔEGFR cells (middle and right).

ΔEGFR. To disrupt miR-9 expression, we first used 5′ RACE to map the host gene of pri-miR-9-2 in U87 cells (Supplementary Fig. S4A). The pri-miR-9-2 host gene was identified to be the large intergenic non-coding RNA, LINC00461 variant 1. Silencing of LINC00461 variant 1 downregulated miR-9 expression and thus confirmed that LINC00461 variant 1 is processed to give rise to miR-9 (Supplementary Fig. S4B). Silencing LINC00461 variant 1 significantly accelerated tumor growth relative to control tumors (Supplementary Fig. S4C). To directly confirm that miR-9 negatively regulates tumorigenicity, U87miRZip control cells and U87miRZip miR-9 cells, showing impaired miR-9 function (Fig. 4C), were implanted into nude mice. Inhibition of miR-9 significantly increased the tumor growth rate of U87 cells (Fig. 5B), showing that miR-9 negatively regulates glioblastoma tumorigenicity.

Repression of FOXP1 by miR-9 appeared to be an attractive mechanism by which miR-9 antagonizes the tumor growth advantage conferred by ΔEGFR (Fig. 5A), because upregulation of miR-9 represses FOXP1 in ΔEGFR cells (Fig. 4B) and disruption of miR-9 activity upregulated FOXP1 (Fig. 4C), and consequently, increased tumorigenicity (Fig. 5B). Support for this was obtained by demonstrating that knockdown of FOXP1

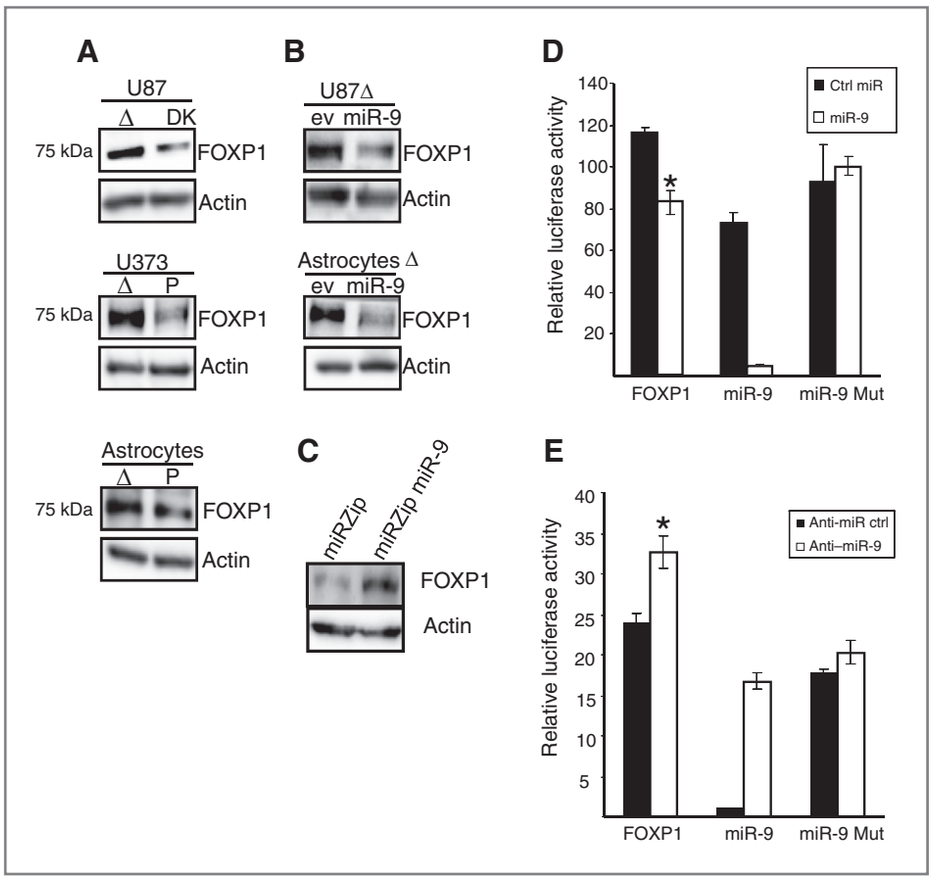

Figure 4. MiR-9 targets FOXP1. A, FOXP1 expression inversely correlates with miR-9 expression. Parental and DK cells with higher miR-9 expression exhibit decreased FOXP1 protein levels relative to ΔEGFR cells showing low miR-9 expression. B, overexpression of miR-9 in U87Δ and astrocytes Δ downregulate FOXP1 expression. C, inhibition of miR-9 activity using the miRZipmiR-9 vector upregulates FOXP1. D, U87ΔEGFR cells were cotransfected with control or miR-9 mimics and FOXP1 3′ UTR luciferase reporter, miR-9, and mutant miR-9 reporters. miR-9 mimics repressed the FOXP1 and miR-9 reporters (*, $P \leq 0.02$) but not the mutant miR-9 reporters. E, U373 cells were cotransfected with anti–miR-9 oligonucleotides and the FOXP1 3′ UTR luciferase reporter, miR-9, and mutant miR-9 reporters. Inhibition of miR-9 activity relieved the repression of FOXP1 and miR-9 reporters (*, $P \leq 0.03$).

using two shRNAs dramatically inhibited the growth of U87ΔEGFR tumors (Fig. 5C and Supplementary Fig. S5). Overexpression of FOXP1 increased the tumorigenic capacity of both U373 and U251 cells demonstrating that FOXP1 is sufficient to enhance tumor growth (Fig. 5D). The significance of this finding is underscored by the significant ($P \leq$ 3.9e-06) correlation of high FOXP1 expression with poor survival in a cohort of 131 patients with glioblastoma (Fig. 5E).

Discussion

In this report, we sought to determine the role of miRNAs in mediating several of the pathogenic effects induced by aberrant EGFR signaling in glioblastoma. Although WTEGFR and ΔEGFR share the same cytoplasmic signaling domains, ΔEGFR, but not WTEGFR, repressed miR-9. Underlining the specificity of this, the activation of several other growth factor receptor tyrosine kinases also had no effect on miR-9. It is likely that persistent signaling from ΔEGFR, as a result of its slow rate of internalization, is involved in the preferential suppression of miR-9 by this mutant receptor (36). Supporting the role of persistent pathway activation in suppressing miR-9, mutant H-Ras G12V alone was sufficient to repress miR-9. Analysis of the TCGA glioblastoma dataset showed decreased miR-9 expression preferentially in glioblastomas with a mesenchymal expression signature and known to show loss, mutation, and/or decreased expression of the negative regulator of Ras, neurofibromin (37). Those glioblastomas with a classical signature and that harbor EGFR amplification and mutants such as ΔEGFR, did not show suppression of miR-9. Because exon arrays lack the sensitivity to reliably detect ΔEGFR in classical glioblastoma samples that coexpress WTEGFR and ΔEGFR, correlations between miR-9 expression levels and ΔEGFR expression are predicted to be imprecise. As well, the heterogeneous expression of WTEGFR and ΔEGFR (9) limit the sensitivity in detecting low miR-9 expression in classical glioblastomas. In support of our observation that WTEGFR does not repress miR-9, we found that classical glioblastoma samples did not display low miR-9 expression.

As activation of the PI3K/AKT axis is more robustly induced by ΔEGFR than by WTEGFR, we examined the pathway components downstream of ΔEGFR and Ras required for repressing miR-9 (38, 39) and found that the PI3K/AKT signaling axis is obligatory. Ras-mediated induction of c-Myc positively regulated miR-9 transcription in breast and neuroblastoma cells (16) and the Ras/Myc/miR-9 axis promoted breast cancer metastasis. Highlighting the importance of the Ras/ERK/c-Myc axis in regulating miR-9, c-Myc was shown to positively regulate miR-9 in multiple tumor models (16, 40, 41), and constitutively active EGFR mutants in lung cancer cells require the Ras/ERK/c-Myc axis to positively regulate miR-9 (42). Collectively, these studies implicate Ras as a key regulator of miR-9 levels in cancer.

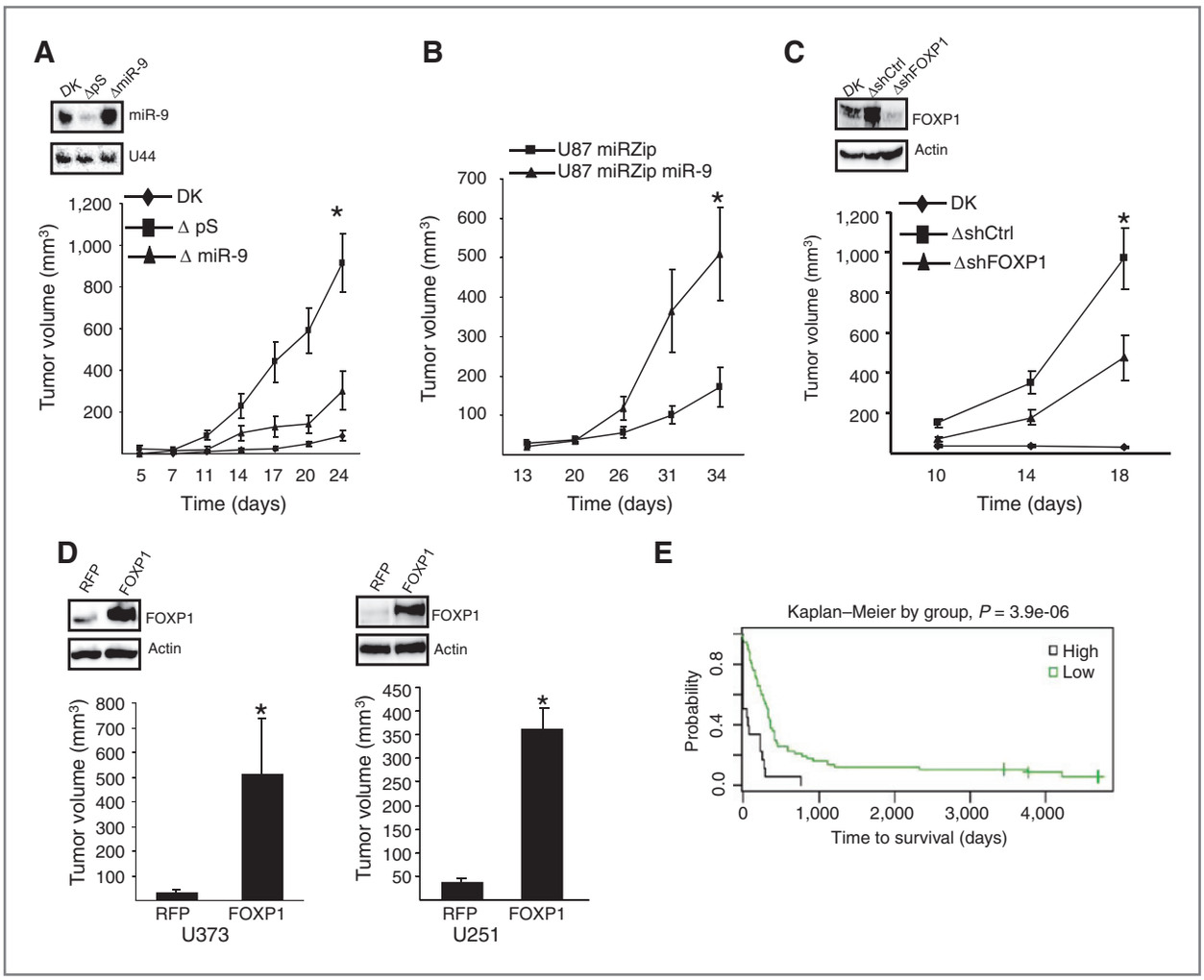

Figure 5. miR-9 and FOXP1 regulate tumorigenicity. A, U87ΔEGFR cells were infected with pSuper vector (pS) and pSmiR-9-1 vector to upregulate miR-9 (top). Mice were subcutaneously implanted with U87DK, U87ΔpS, and U87ΔmiR-9 cells. The growth of U87DK and U87ΔmiR-9 tumors was significantly slower compared with U87ΔpS tumors (*, $P \leq 0.01$). B, mice implanted with U87miRZip control cells developed significantly smaller tumors relative to mice implanted with U87miRZip miR-9 cells showing impaired miR-9 activity (*, $P \leq 0.03$). C, knockdown of FOXP1 dramatically impaired the growth of U87ΔEGFR tumors (*, $P \leq 0.02$). D, overexpression of FOXP1 increases the tumorigenic capacity of U373 and U251 cells (*, $P \leq 0.02$). E, Kaplan–Meier survival curve analysis reveals that high FOXP1 predicts poor survival in a cohort of 131 patients with glioblastoma.

The repression of miR-9 by ΔEGFR suggested that miR-9 is a tumor suppressor. Consistent with this, miR-9 inhibited the growth of ΔEGFR-dependent tumors and inhibition of miR-9 activity enhanced tumor growth. Jeon and colleagues reported that ID4 inhibited miR-9* expression to promote chemoresistance, glioma self-renewal and tumorigenicity by induction of the miR-9* target, SOX-2 (32). In glioblastoma $CD133^+$ stem cells, miR-9 and miR-9* were highly expressed and required for glioblastoma stem cell renewal (43). Interestingly, miR-9 and miR-9* acted in a cooperative manner to repress the novel tumor suppressor, CAMTA1 (43). We identified the transcription factor, FOXP1, as a novel miR-9 target in glioblastoma cells, in which their expression was inversely correlated. Correspondingly, the induction of FOXP1 by inhibition of miR-9 increased tumor growth, while knockdown of FOXP1 inhibited the growth of ΔEGFR tumors. Our data suggest that FOXP1 is a likely tumor-promoting factor in glioblastoma.

Overexpression of FOXP1 confers a poor prognosis to lymphoma (44) and hepatocellular carcinoma patients (45), suggesting that FOXP1 is an oncogene. However, in breast cancer (46) and T-cell lymphomas (47), FOXP1 expression is associated with favorable outcomes, suggesting a possible tissue-specific role as a tumor suppressor. FOXP1 increases the proliferation of the ERα-positive breast cancer cell line, MCF-7, suggesting that FOXP1 serves as a surrogate marker for ER-dependent breast cancers (48). FOXP1 expression is restricted to neurons within different regions of the brain (49, 50). As we observed FOXP1 expression in tumors of glial lineage, it is plausible that FOXP1 induction is required for the dedifferentiation of astrocytes to multipotent stem cell–like progenitors during the gliomagenesis process in the setting

of oncogenic ΔEGFR signaling. Given that miR-9 expression is higher in the minority CD133$^+$ stem cell compartment of glioblastomas (43), low miR-9 expression might induce FOXP1 to provide for a rapid and lethal expansion of the non–stem cell compartment. The role we have uncovered for FOXP1 and its transcriptional targets may yield novel therapeutic approaches and targets to improve survival of patients with glioblastoma.

Disclosure of Potential Conflicts of Interest

No potential conflicts of interest were disclosed.

Authors' Contributions

Conception and design: G.G. Gomez, F.B. Furnari, W.K. Cavenee
Development of methodology: G.G. Gomez, D.H. Gutmann, C.W. Brennan
Acquisition of data (provided animals, acquired and managed patients, provided facilities, etc.): G.G. Gomez, C.M. Croce, C. Zanca, M. Li
Analysis and interpretation of data (e.g., statistical analysis, biostatistics, computational analysis): G.G. Gomez, S. Volinia, R. Emnett, D.H. Gutmann, C. W. Brennan, F.B. Furnari, W.K. Cavenee
Writing, review, and/or revision of the manuscript: G.G. Gomez, S. Volinia, C. Zanca, D.H. Gutmann, C.W. Brennan, F.B. Furnari, W.K. Cavenee
Administrative, technical, or material support (i.e., reporting or organizing data, constructing databases): G.G. Gomez, R. Emnett, W.K. Cavenee
Study supervision: F.B. Furnari, W.K. Cavenee

Acknowledgments

The authors thank Dr. Tomoyuki Koga (Ludwig Institute for Cancer Research) for providing statistical analyses, Dr. Eliezer Masliah and Kori Kosberg in the UCSD Department of Neurosciences for providing pLV-hFOXP1 lentiviral stocks, and Dr. David E. Root, Director of the RNAi Platform and The RNAi Consortium at the Broad Institute of MIT and Harvard, for the design of shRNA used to target LINC40061.

Grant Support

This study was supported by an American Brain Tumor Association Basic Research grant to G.G. Gomez in memory of Keith Powers, P01-CA95616 (W.K. Cavenee, F.B. Furnari), R01-NS080939 and James S. McDonnell Foundation (F.B. Furnari). W.K. Cavenee is a Fellow of the National Foundation for Cancer Research. S. Volinia is recipient of AIRC IG13585 grant.

The costs of publication of this article were defrayed in part by the payment of page charges. This article must therefore be hereby marked *advertisement* in accordance with 18 U.S.C. Section 1734 solely to indicate this fact.

Received July 24, 2013; revised November 22, 2013; accepted December 9, 2013; published OnlineFirst January 16, 2014.

References

1. Dunn GP, Rinne ML, Wykosky J, Genovese G, Quayle SN, Dunn IF, et al. Emerging insights into the molecular and cellular basis of glioblastoma. Genes Dev 2012;26:756–84.
2. Nishikawa R, Sugiyama T, Narita Y, Furnari F, Cavenee WK, Matsutani M. Immunohistochemical analysis of the mutant epidermal growth factor, deltaEGFR, in glioblastoma. Brain Tumor Pathol 2004;21:53–6.
3. Sugawa N, Ekstrand AJ, James CD, Collins VP. Identical splicing of aberrant epidermal growth factor receptor transcripts from amplified rearranged genes in human glioblastomas. Proc Natl Acad Sci U S A 1990;87:8602–6.
4. Lammering G, Valerie K, Lin PS, Hewit TH, Schmidt-Ullrich RK. Radiation-induced activation of a common variant of EGFR confers enhanced radioresistance. Radiother Oncol 2004;72:267–73.
5. Nagane M, Levitzki A, Gazit A, Cavenee WK, Huang HJ. Drug resistance of human glioblastoma cells conferred by a tumor-specific mutant epidermal growth factor receptor through modulation of Bcl-XL and caspase-3-like proteases. Proc Natl Acad Sci U S A 1998; 95:5724–9.
6. Li M, Mukasa A, Inda MM, Zhang J, Chin L, Cavenee W, et al. Guanylate binding protein 1 is a novel effector of EGFR-driven invasion in glioblastoma. J Exp Med 2011;208:2657–73.
7. Nishikawa R, Ji XD, Harmon RC, Lazar CS, Gill GN, Cavenee WK, et al. A mutant epidermal growth factor receptor common in human glioma confers enhanced tumorigenicity. Proc Natl Acad Sci U S A 1994; 91:7727–31.
8. Mukasa A, Wykosky J, Ligon KL, Chin L, Cavenee WK, Furnari F. Mutant EGFR is required for maintenance of glioma growth in vivo, and its ablation leads to escape from receptor dependence. Proc Natl Acad Sci U S A 2010;107:2616–21.
9. Inda MM, Bonavia R, Mukasa A, Narita Y, Sah DW, Vandenberg S, et al. Tumor heterogeneity is an active process maintained by a mutant EGFR-induced cytokine circuit in glioblastoma. Genes Dev 2010;24: 1731–45.
10. Ambros V, Bartel B, Bartel DP, Burge CB, Carrington JC, Chen X, et al. A uniform system for microRNA annotation. RNA 2003;9: 277–9.
11. Han J, Lee Y, Yeom KH, Kim YK, Jin H, Kim VN. The Drosha-DGCR8 complex in primary microRNA processing. Genes Dev 2004;18: 3016–27.
12. Yi R, Qin Y, Macara IG, Cullen BR. Exportin-5 mediates the nuclear export of pre-microRNAs and short hairpin RNAs. Genes Dev 2003;17: 3011–6.
13. Grishok A, Pasquinelli AE, Conte D, Li N, Parrish S, Ha I, et al. Genes and mechanisms related to RNA interference regulate expression of the small temporal RNAs that control C. elegans developmental timing. Cell 2001;106:23–34.
14. Mourelatos Z, Dostie J, Paushkin S, Sharma A, Charroux B, Abel L, et al. miRNPs: a novel class of ribonucleoproteins containing numerous microRNAs. Genes Dev 2002;16:720–8.
15. Calin GA, Croce CM. MicroRNA signatures in human cancers. Nat Rev Cancer 2006;6:857–66.
16. Ma L, Young J, Prabhala H, Pan E, Mestdagh P, Muth D, et al. miR-9, a MYC/MYCN-activated microRNA, regulates E-cadherin and cancer metastasis. Nat Cell Biol 2010;12:247–56.
17. Papagiannakopoulos T, Friedmann-Morvinski D, Neveu P, Dugas JC, Gill RM, Huillard E, et al. Pro-neural miR-128 is a glioma tumor suppressor that targets mitogenic kinases. Oncogene 2012;31: 1884–95.
18. Kefas B, Godlewski J, Comeau L, Li Y, Abounader R, Hawkinson M, et al. microRNA-7 inhibits the epidermal growth factor receptor and the Akt pathway and is down-regulated in glioblastoma. Cancer Res 2008; 68:3566–72.
19. Guessous F, Zhang Y, Kofman A, Catania A, Li Y, Schiff D, et al. microRNA-34a is tumor suppressive in brain tumors and glioma stem cells. Cell Cycle 2010;9:1031–6.
20. Shao M, Rossi S, Chelladurai B, Shimizu M, Ntukogu O, Ivan M, et al. PDGF induced microRNA alterations in cancer cells. Nucleic Acids Res 2011;39:4035–47.
21. Prigent SA, Nagane M, Lin H, Huvar I, Boss GR, Feramisco JR, et al. Enhanced tumorigenic behavior of glioblastoma cells expressing a truncated epidermal growth factor receptor is mediated through the Ras-Shc-Grb2 pathway. J Biol Chem 1996;271:25639–45.
22. Bachoo RM, Maher EA, Ligon KL, Sharpless NE, Chan SS, You MJ, et al. Epidermal growth factor receptor and Ink4a/Arf: convergent mechanisms governing terminal differentiation and transformation along the neural stem cell to astrocyte axis. Cancer Cell 2002;1: 269–77.
23. Yeh TH, Lee da Y, Gianino SM, Gutmann DH. Microarray analyses reveal regional astrocyte heterogeneity with implications for neurofibromatosis type 1 (NF1)-regulated glial proliferation. Glia 2009;57: 1239–49.
24. Liu CG, Calin GA, Meloon B, Gamliel N, Sevignani C, Ferracin M, et al. An oligonucleotide microchip for genome-wide microRNA profiling in human and mouse tissues. Proc Natl Acad Sci U S A 2004;101:9740–4.

25. Bazzoni F, Rossato M, Fabbri M, Gaudiosi D, Mirolo M, Mori L, et al. Induction and regulatory function of miR-9 in human monocytes and neutrophils exposed to proinflammatory signals. Proc Natl Acad Sci U S A 2009;106:5282–7.
26. Nagane M, Coufal F, Lin H, Bogler O, Cavenee WK, Huang HJ. A common mutant epidermal growth factor receptor confers enhanced tumorigenicity on human glioblastoma cells by increasing proliferation and reducing apoptosis. Cancer Res 1996;56:5079–86.
27. Avraham R, Sas-Chen A, Manor O, Steinfeld I, Shalgi R, Tarcic G, et al. EGF decreases the abundance of microRNAs that restrain oncogenic transcription factors. Sci Signal 2010;3:ra43.
28. Karsy M, Arslan E, Moy F. Current progress on understanding MicroRNAs in glioblastoma multiforme. Genes Cancer 2012;3:3–15.
29. Moscatello DK, Holgado-Madruga M, Emlet DR, Montgomery RB, Wong AJ. Constitutive activation of phosphatidylinositol 3-kinase by a naturally occurring mutant epidermal growth factor receptor. J Biol Chem 1998;273:200–6.
30. Suzuki HI, Yamagata K, Sugimoto K, Iwamoto T, Kato S, Miyazono K. Modulation of microRNA processing by p53. Nature 2009;460:529–33.
31. Dasgupta B, Li W, Perry A, Gutmann DH. Glioma formation in neurofibromatosis 1 reflects preferential activation of K-RAS in astrocytes. Cancer Res 2005;65:236–45.
32. Jeon HM, Sohn YW, Oh SY, Kim SH, Beck S, Kim S, et al. ID4 imparts chemoresistance and cancer stemness to glioma cells by derepressing miR-9*-mediated suppression of SOX2. Cancer Res 2011;71:3410–21.
33. Kim TM, Huang W, Park R, Park PJ, Johnson MD. A developmental taxonomy of glioblastoma defined and maintained by MicroRNAs. Cancer Res 2011;71:3387–99.
34. Yang JH, Li JH, Shao P, Zhou H, Chen YQ, Qu LH. starBase: a database for exploring microRNA-mRNA interaction maps from Argonaute CLIP-Seq and Degradome-Seq data. Nucleic Acids Res 2011;39:D202–9.
35. Otaegi G, Pollock A, Hong J, Sun T. MicroRNA miR-9 modifies motor neuron columns by a tuning regulation of FoxP1 levels in developing spinal cords. J Neurosci 2011;31:809–18.
36. Huang HS, Nagane M, Klingbeil CK, Lin H, Nishikawa R, Ji XD, et al. The enhanced tumorigenic activity of a mutant epidermal growth factor receptor common in human cancers is mediated by threshold levels of constitutive tyrosine phosphorylation and unattenuated signaling. J Biol Chem 1997;272:2927–35.
37. Verhaak RG, Hoadley KA, Purdom E, Wang V, Qi Y, Wilkerson MD, et al. Integrated genomic analysis identifies clinically relevant subtypes of glioblastoma characterized by abnormalities in PDGFRA, IDH1, EGFR, and NF1. Cancer Cell 2010;17:98–110.
38. Schmidt MH, Furnari FB, Cavenee WK, Bogler O. Epidermal growth factor receptor signaling intensity determines intracellular protein interactions, ubiquitination, and internalization. Proc Natl Acad Sci U S A 2003;100:6505–10.
39. Huang PH, Miraldi ER, Xu AM, Kundukulam VA, Del Rosario AM, Flynn RA, et al. Phosphotyrosine signaling analysis of site-specific mutations on EGFRvIII identifies determinants governing glioblastoma cell growth. Mol Biosyst 2010;6:1227–37.
40. Sun Y, Wu J, Wu SH, Thakur A, Bollig A, Huang Y, et al. Expression profile of microRNAs in c-Myc induced mouse mammary tumors. Breast Cancer Res Treat 2009;118:185–96.
41. Onnis A, De Falco G, Antonicelli G, Onorati M, Bellan C, Sherman O, et al. Alteration of microRNAs regulated by c-Myc in Burkitt lymphoma. PLoS One 2010;5.
42. Kang HW, Crawford M, Fabbri M, Nuovo G, Garofalo M, Nana-Sinkam SP , et al. A mathematical model for microRNA in lung cancer. PLoS One 2013;8:e53663.
43. Schraivogel D, Weinmann L, Beier D, Tabatabai G, Eichner A, Zhu JY, et al. CAMTA1 is a novel tumour suppressor regulated by miR-9/9* in glioblastoma stem cells. EMBO J 2011;30:4309–22.
44. Zhai L, Zhao Y, Ye S, Huang H, Tian Y, Wu Q, et al. Expression of PIK3CA and FOXP1 in gastric and intestinal non-Hodgkin's lymphoma of mucosa-associated lymphoid tissue type. Tumour Biol 2011;32:913–20.
45. Zhang Y, Zhang S, Wang X, Liu J, Yang L, He S, et al. Prognostic significance of FOXP1 as an oncogene in hepatocellular carcinoma. J Clin Pathol 2012;65:528–33.
46. Ijichi N, Shigekawa T, Ikeda K, Horie-Inoue K, Shimizu C, Saji S, et al. Association of double-positive FOXA1 and FOXP1 immunoreactivities with favorable prognosis of tamoxifen-treated breast cancer patients. Horm Cancer 2012;3:147–59.
47. Yamada S, Sato F, Xia H, Takino H, Kominato S, Ri M, et al. Forkhead box P1 overexpression and its clinicopathologic significance in peripheral T-cell lymphoma, not otherwise specified. Hum Pathol 2012;43:1322–7.
48. Shigekawa T, Ijichi N, Ikeda K, Horie-Inoue K, Shimizu C, Saji S, et al. FOXP1, an estrogen-inducible transcription factor, modulates cell proliferation in breast cancer cells and 5-year recurrence-free survival of patients with tamoxifen-treated breast cancer. Horm Cancer 2011;2:286–97.
49. Ferland RJ, Cherry TJ, Preware PO, Morrisey EE, Walsh CA. Characterization of Foxp2 and Foxp1 mRNA and protein in the developing and mature brain. J Comp Neurol 2003;460:266–79.
50. Tamura S, Morikawa Y, Iwanishi H, Hisaoka T, Senba E. Foxp1 gene expression in projection neurons of the mouse striatum. Neuroscience 2004;124:261–7.